Philippine Journal of Science
149 (2): 325-333, June 2020
ISSN 0031 - 7683
Date Received: 22 Oct 2019

Preparation and Characterization of an Amino-functionalized α-Cellulose from Pineapple [*Ananas comosus* (L.) Merr.] Crown Leaves

Ralph Lauren M. Alomia[1]*, **Veronica C. Sabularse**[1], **Marivic S. Lacsamana**[1], **Ramon A. Razal**[2], and **Hidelisa P. Hernandez**[1]

[1]Institute of Chemistry, College of Arts and Sciences
[2]Department of Forest Products and Paper Science, College of Forestry and Natural Resources
University of the Philippines Los Baños, College, Laguna 4031 Philippines

Amino-functionalized α-cellulose from pineapple [*Ananas comosus* (L.) Merr.] crown leaves (PCLs) was prepared using 3-(aminopropyl)triethoxysilane (APTES) to explore the diverse utilization of PCL. It was then characterized using optical microscopy, attenuated total reflectance Fourier-transform infrared spectroscopy (ATR FTIR), ninhydrin test, and differential scanning calorimetry (DSC). The amino-functionalization was confirmed by the appearance of disintegrated primary layers and balloons in the 400x and 1000x optical micrographs, higher lateral order index (LOI), higher total crystallinity index (TCI), higher energy of H-bonds (E_H) at 3432 cm^{-1}, longer radius of H-bonds (R) at 3432 cm^{-1}, higher depolymerization temperature ($T_{m(DP)}$), and higher enthalpy of dehydration ($\Delta_{dehydration}H$) of α-cellulose-APTES as compared to α-cellulose, and the positive reaction of α-cellulose-APTES with ninhydrin. The results showed that the prepared α-cellulose-APTES have notable properties to be used in a variety of adsorbent and enzyme-immobilization applications.

Keywords: amino-functionalization, pineapple crown leaves, α-cellulose, α-cellulose-APTES

INTRODUCTION

Pineapple [*Ananas comosus* (L.) Merr.] crown leaves (PCL) is one of the by-products of pineapple fruit processing (Upadhyay *et al.* 2010). Compared to pineapple slips and suckers, PCL is not used for propagation and is usually disposed of. According to Ban-Koffi and Han (1990), around 40–80% of pineapple fruit is discarded as waste, and the disposal of these wastes has a negative impact on our environment due to its high biological oxygen demand and chemical oxygen demand.

Most literature on the utilization of pineapple wastes deals with the extraction and application of pineapple leaf fibers (PALF). PALF has been reported to have excellent mechanical properties appropriate for the production of polymer composites (Asim *et al.* 2015). Compared to PALF, PCL also has significant amounts of cellulose. According to Tran (2006), PCL mostly contains holocellulose (34.3%), lignin (23.3%), and α-cellulose (19.1%). Due to this chemical composition, PCL has been used for pulp and paper production (Tran 2006). Recently, Prado and Spinace (2019) successfully extracted cellulose nanocrystals from PCL by alkali treatment followed by acid hydrolysis. Also, PCL has been used for the extraction of hemicelluloses, yielding substantial amounts of mercerized α-cellulose. Hence, there is a need to study the utilization of these byproducts.

The structure of α-cellulose can be modified to enhance its reactivity and to maximize its utilization. The low

*Corresponding Author: rmalomia@up.edu.ph

reactivity is due to the intra- and intermolecular hydrogen bonds among the hydroxyl groups (-OH) (Rowell *et al.* 2012) and steric effects (Hebeish and Guthrie 1981). One way to improve the physical and chemical properties of cellulose is through amino-functionalization. Compared to the hydroxyl groups in cellulose, the amino groups can be easily protonated by acids resulting in the formation of cationic moieties (Liesiene and Kazlauske 2013). Also, they can easily bind with the amino groups in proteins using glutaraldehyde as a coupling agent (Barbosa *et al.* 2014). Amino-functionalized cellulose was reported to have potential applications as an adsorbent for the removal of Cu^{2+} (Wu *et al.* 2019) and anionic dyes (Silva *et al.* 2018) in water and as support for the immobilization of horseradish peroxidase (Yu *et al.* 2019).

In this study, the amino-functionalization of α-cellulose from PCL using APTES was investigated by optical microscopy, ATR FTIR spectroscopy, ninhydrin test, and DSC.

MATERIALS AND METHODS

Materials

The alkaline residue from the extraction of hemicellulose from PCL provided by the University of the Philippines Los Baños – Institute of Chemistry Fruit Coating Research Group (UPLB-IC FCRG) was treated with hot-water to a constant pH of 10 to remove impurities and excess NaOH. From this, mercerized cellulose with 0.972 ± 0.011% (n = 3) (oven-dry basis) acid-insoluble lignin was obtained. Then, the mercerized cellulose was neutralized with 1% acetic acid to recover α-cellulose. The 98.0% APTES used in the preparation of α-cellulose-APTES was supplied by Sigma-Aldrich®, USA.

Preparation of α-cellulose-APTES

In a 125-mL Erlenmeyer flask, about 0.50 g of oven-dried α-cellulose was suspended in 40 mL 3:1 acetonitrile-distilled H_2O, sonicated for 1 h in a cold bath, and stirred for another hour at room temperature. The sonicated mixture was then transferred to a 100-mL polypropylene beaker covered with a watch glass and stirred constantly for 2 h at 50–80 °C. While stirring, 600 µL of 98.0% APTES was gradually added to the reaction mixture. Stirring was continued for 30 min and the resulting suspension was then cooled at room temperature and allowed to stand overnight. After standing, the α-cellulose-APTES product was then filtered in a tared fritted glass crucible with coarse porosity (40–60 µm). The product collected was washed with 15-mL portions of distilled H_2O until the filtrate had no appreciable reaction with 2% ninhydrin in isopropyl alcohol, washed with 15 mL isopropyl alcohol, and suction-filtered. The washed α-cellulose-APTES product was then oven-dried at 105 °C for 3 h.

Characterization of α-cellulose and α-cellulose-APTES

The α-cellulose and α-cellulose-APTES were characterized through optical microscopy, ATR FTIR, DSC, and wet chemical analysis. Moreover, the degree of substitution (DS) of α-cellulose-APTES was determined by acid-base titrimetry. The samples used for each analysis were oven-dried for 10 h at 80 °C, cooled in a desiccator, and stored for at most one day in screw-capped vials. During storage, the vials were placed in a Ziploc® bag containing silica gel as desiccant.

Determination of the DS of α-cellulose-APTES. A similar procedure used by Jung *et al.* (2012) for the quantitative determination of amine sites on modified SiO_2 nanoparticles was applied to determine the DS of α-cellulose-APTES. In a 50-mL Erlenmeyer flask, about 0.01 g of α-cellulose-APTES was suspended in 20.00 mL distilled water and sonicated in an ice bath for 30 min. Ten (10) mL of 1.243 mM HCl solution was added to 10.00 mL of the suspension, and the mixture was swirled vigorously. The mixture was then titrated with 0.9194 mM NaOH solution up to the phenolphthalein endpoint. The DS was computed using Equation 1:

$$DS = \frac{(C_{HCl}V_{HCl} - C_{NaOH}V_{NaOH})(MM_{glucose})}{(w_{ca(OD)})} \quad (1)$$

where $w_{ca(OD)}$ is the oven-dried weight of α-cellulose-APTES, C_{HCl} is the molar concentration of standardized HCl solution, C_{NaOH} is the molar concentration of standardized NaOH solution, V_{HCl} is the volume of standardized HCl solution in L, and V_{NaOH} is the volume of standardized NaOH solution in L. The determination of the DS of α-cellulose-APTES was done in triplicate.

Optical microscopy. The 400x and 1000x magnification optical micrographs of α-cellulose and α-cellulose-APTES were obtained using the OPTIKA® B-383PLi trinocular microscope (Italy) equipped with OptikamB5 digital camera 4083.B5 through the OptikalSview® software.

In the preparation of microscope slides, a suspension of 0.1 g sample in 10 mL water was sonicated for 30 min. Afterward, a drop of the resulting suspension was mounted on a microscope slide with a coverslip. Lastly, the slides were oven-dried at 105 °C for 30 min.

ATR FTIR spectroscopy. The FTIR spectra of α-cellulose and α-cellulose-APTES were obtained using the Shimadzu® IR Prestige-21 FTIR Spectrophotometer

(Japan) equipped with Single Reflection ATR Accessory through the Shimadzu IRsolution® software. The FTIR transmittance spectra of α-cellulose and α-cellulose-APTES were compared to determine the structural changes brought about by the attachment of APTES in α-cellulose.

Crystallinity parameters such as LOI (Equation 2), TCI (Equation 3), and hydrogen bond intensity (HBI) (Equation 4) of α-cellulose and α-cellulose-APTES were calculated from their corresponding FTIR absorbance spectra. The determination of each parameter was done in quadruplicate.

$$LOI = \frac{A_{1425\ cm^{-1}}}{A_{898\ cm^{-1}}} \qquad (2)$$

$$TCI = \frac{A_{1372\ cm^{-1}}}{A_{2900\ cm^{-1}}} \qquad (3)$$

$$HBI = \frac{A_{3400\ cm^{-1}}}{A_{1320\ cm^{-1}}} \qquad (4)$$

Moreover, various hydrogen bonds in α-cellulose and α-cellulose-APTES were assessed by calculating the energy (E_H) (Equation 5), and distance (R) (Equation 6). These were done by determining the nearest frequency of absorptions at 3567 cm^{-1} [lignin ArOH *(intra)*] (Popescu *et al.* 2011), 3432 cm^{-1} [cellulose I and II O2-H---O6' *(intra)*] (Kondo 1997; Oh *et al.* 2005), 3342 cm^{-1} [cellulose I and II O3-H---O5' (*intra*)] (Kondo 1997), 3278 cm^{-1} [cellulose I_β O6-H---O3' *(inter)*] (Oh *et al.* 2005), and 3221 cm^{-1} [cellulose I_α O6-H---O3' *(inter)*] (Oh *et al.* 2005; Popescu *et al.* 2011) in the 2nd derivative FTIR absorbance spectra of each sample:

$$E_H = \left(\frac{1}{k}\right)\left(\frac{v_o - v}{v_o}\right) \qquad (5)$$

where k is a constant (1/k = 2.625 x 10^2 kJ), v_o is the frequency corresponding to the free hydroxyl groups (3650 cm^{-1}), and v is the frequency of the bonded hydroxyl groups (observed).

$$R = 2.84 - \left(\frac{v_o - v}{4430}\right) \qquad (6)$$

where v_o is the frequency corresponding to the monomeric hydroxyl stretch (3600 cm^{-1}), and v is the stretching frequency of the hydroxyl groups (observed). The determination of E_H and R in each type of hydrogen bond was done in quadruplicate.

The significant differences at 95% confidence level among α-cellulose and α-cellulose-APTES for each parameter derived from ATR FTIR spectroscopy were determined through the one-way analysis of variance (ANOVA) and Tukey's multiple comparisons test. The statistical analysis was performed using the GraphPad Prism® version 7 software.

DSC. The DSC thermograms of α-cellulose and α-cellulose-APTES were obtained using TA Instruments® Differential Scanning Calorimeter Q20 (USA). Each sample was pre-weighed in a T_{zero} aluminum pan and subjected to DSC analysis by measuring the heat flow (W/g) from 25–350 °C at a rate of 3 °C/min. Afterward, the dehydration and depolymerization temperatures (T_m), glass transition temperatures (T_g), and the change in enthalpies were determined from the DSC thermograms through the Universal® version 4.5 software.

Ninhydrin test. The presence of the amino-functional group in α-cellulose-APTES was confirmed by the ninhydrin test. In a test tube covered with parafilm, about 1 mg sample was suspended in 1 mL 2% ninhydrin in isopropyl alcohol for 3 h. Afterward, the color of the fibers and the supernatant liquid was observed.

RESULTS

Determination of the DS of α-cellulose-APTES

The α-cellulose-APTES prepared from the reaction of mercerized cellulose with APTES was found to have a DS of 0.01041 ± 0.0008 (n = 3).

Optical Microscopy

The 400x and 1000x optical micrographs of α-cellulose and α-cellulose-APTES were also obtained (Figure 1). The dispersal of fibrils was more pronounced in α-cellulose-

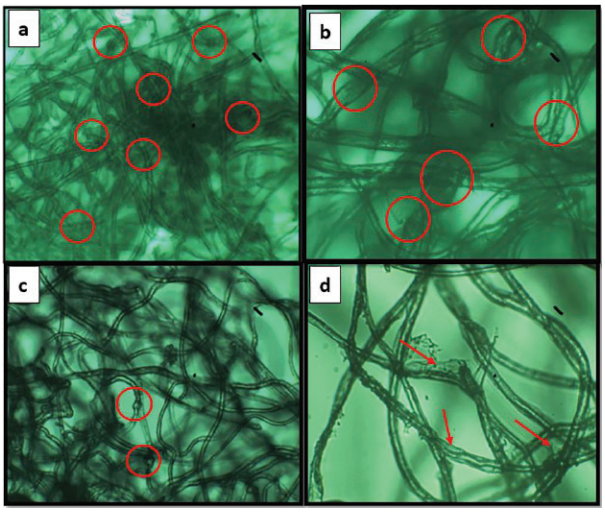

Figure 1. The optical micrographs of α-cellulose (a: 400x; b: 1000x) and α-cellulose-APTES (c: 400x; d: 1000x). The red circles indicate the balloons while the red arrows point to the disintegrated primary layers.

APTES than in α-cellulose. Ballooning of fibers was observed in both α-cellulose and α-cellulose-APTES but the disintegration of primary layers was evident only in α-cellulose-APTES.

ATR FTIR Spectroscopy

The ATR FTIR transmittance spectra of α-cellulose and α-cellulose-APTES had similar absorption frequencies (Table 1). The FTIR crystallinity parameters such as the LOI, TCI, and HBI of α-cellulose and α-cellulose-APTES (Table 2) were also derived from the corresponding FTIR absorbance spectra. The α-cellulose was found to have a significantly lower LOI and TCI, and similar HBI than α-cellulose-APTES at 95% confidence level. Moreover, the E_H and the R of the hydrogen bonds in α-cellulose and α-cellulose-APTES were derived from their corresponding 2nd derivative absorbance spectra.

Table 1. The observed peaks in the ATR FTIR transmittance spectra of α-cellulose (A) and α-cellulose-APTES (AA) with corresponding peak assignments.

Wave numbers (cm^{-1})		Peak assignments (Oh *et al.* 2005)
A	AA	
3334.92	3332.99	-O-H stretch (hydrogen-bonded)
2891.30	2891.30	C-H stretch
1641.42	1635.64	bound water
1421.54	1419.61	CH_2 symmetric bending at C6
1365.60	1365.60	C-H bending
1313.52	1313.52	CH_2 wagging at C6
1157.29	1157.29	C-O-C stretch at β-glucosidic linkage
1024.20	1020.34	C-O stretch at C6
894.97	894.97	C-O-C stretch at β-glycosidic linkage, C-O-C stretch, C-C-O stretch, and C-C-H stretch at C5 and C6
669.30	667.37	C-O-H out-of-plane bending

Table 2. The FTIR crystallinity parameters of α-cellulose (A) and α-cellulose-APTES (AA).

Sample	FTIR crystallinity parameters		
	LOI*	TCI*	HBI*
A	$0.7178^{a} \pm 0.0096$	$0.5197^{a} \pm 0.0119$	$3.1696^{a} \pm 0.1405$
AA	$0.7693^{b} \pm 0.0314$	$0.5407^{a,b} \pm 0.0150$	$3.1176^{a} \pm 0.1463$

*Means of four determinations: means in the same column with the same superscript letter(s) are not significantly different at 95% confidence level based on one-way ANOVA and Tukey's multiple comparisons test.

The calculated values for E_H and R are summarized in Table 3. At a 95% confidence level, only the E_H and R of the O2-H---O6' intramolecular hydrogen bonds (3432 cm^{-1}) in α-cellulose-APTES were found to be significantly different from those calculated in α-cellulose.

DSC

In the DSC thermograms of α-cellulose and α-cellulose-APTES, there were two endotherms observed at

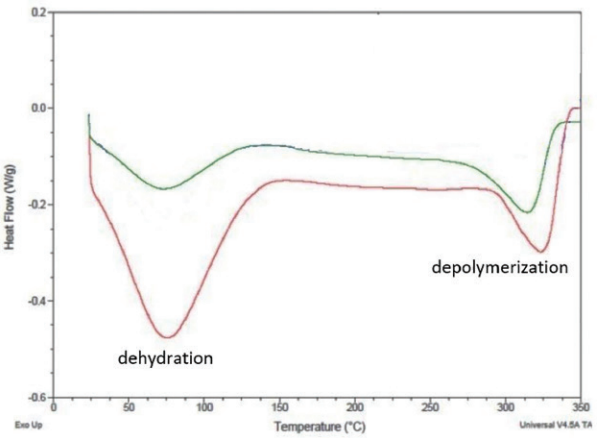

Figure 2. The stacked DSC thermograms of α-cellulose (A) (green) and α-cellulose-APTES (AA) (red).

Table 3. The distance, R (Å) and energy, E_H (kJ) of the various hydrogen bonds in α-cellulose (A) and α-cellulose-APTES (AA).

Sample	Distance, R (Å) and energy, E_H (kJ) of hydrogen bonds									
	3567 cm^{-1} lignin Ar-OH (*intra*)		3432 cm^{-1} O2-H --- O6' (*intra*)		3342 cm^{-1} O3-H --- O5' (*intra*)		3278 cm^{-1} O6-H --- O3' (*inter*)		3221 cm^{-1} O6-H --- O3' (*inter*)	
	R	E_H	R	E_H	R	E_H	R	E_H	R	E_H
A	$2.8322^{a} \pm 0.0008$	$6.0832^{a} \pm 0.2404$	$2.8017^{a} \pm 0.0003$	$15.7935^{a} \pm 0.0801$	$2.7831^{a} \pm 0.0002$	$21.72349^{a} \pm 0.0690$	$2.7661^{a} \pm 0.0013$	$27.1333^{a} \pm 0.4297$	$2.7552^{a} \pm 0.0014$	$30.6010^{a} \pm 0.4583$
AA	$2.8320^{a} \pm 0.0006$	$6.1526^{a} \pm 0.1963$	$2.8005^{b} \pm 0.0004$	$16.1745^{b} \pm 0.1329$	$2.7829^{a} \pm 0.0008$	$21.7925^{a} \pm 0.2624$	$2.7680^{a} \pm 0.0017$	$26.5438^{a} \pm 0.5431$	$2.7559^{a} \pm 0.0004$	$30.3998^{a} \pm 0.1263$

*Means of four determinations: means in the same column with the same superscript letter(s) are not significantly different at 95% confidence level based on one-way ANOVA and Tukey's multiple comparisons test

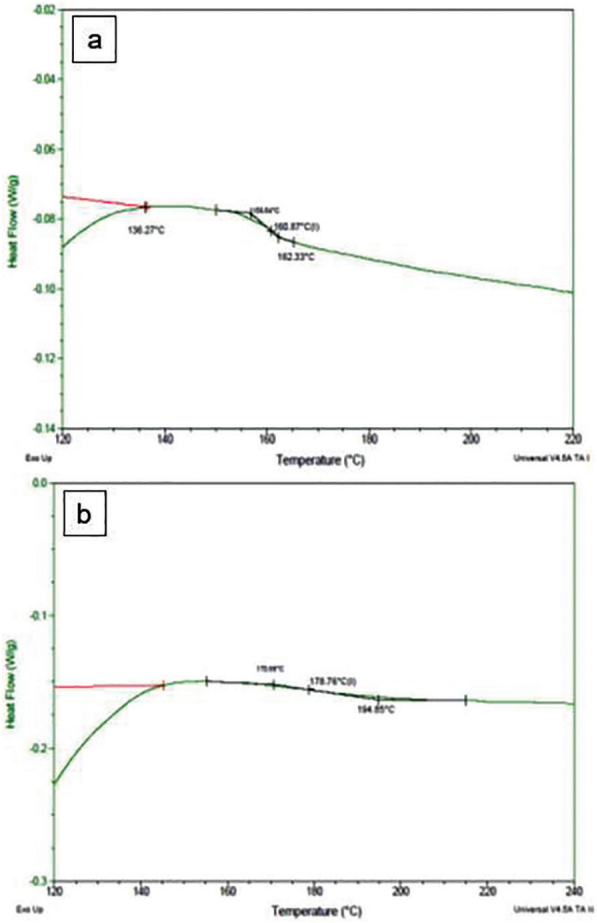

Figure 3. The DSC thermograms of α-cellulose (A) (a) and α-cellulose-APTES (AA) (b) from 120–220 °C showing $T_g(1)$.

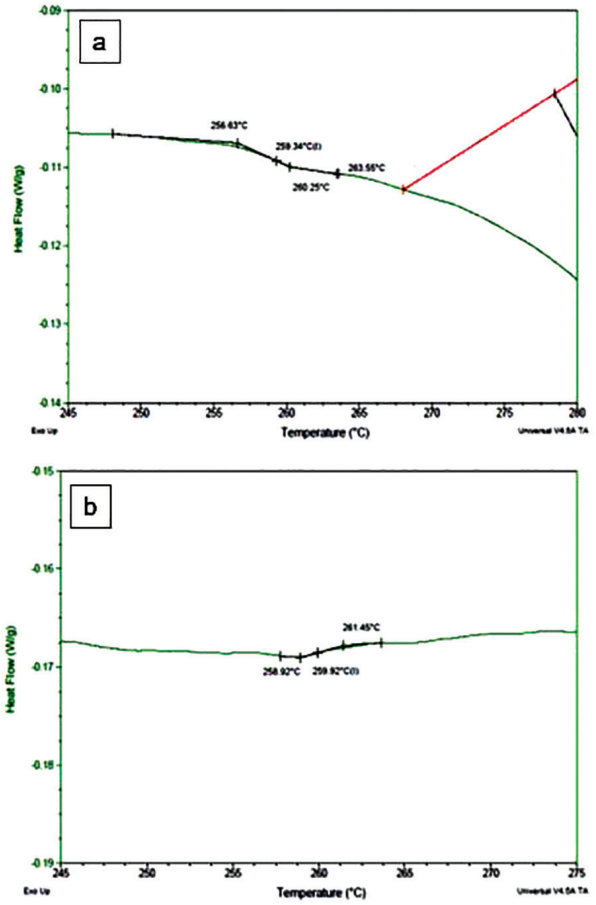

Figure 4. The DSC thermograms of α-cellulose (A) (a) and α-cellulose-APTES (AA) (b) from 245–275 °C showing $T_g(2)$.

Table 4. The thermal properties of α-cellulose (A), and α-cellulose-APTES (AA) derived from their corresponding DSC thermograms.

Sample	Thermal properties					
	Dehydration, $T_{m\,(DH)}$ (°C)	$\Delta_{dehydration}$ H (J/g)	Depolymerization, $T_{m\,(DP)}$ (°C)	$\Delta_{depolymerization}$ H (J/g)	Tg(1) (°C)	Tg(2) (°C)
A	72.28	118.7	315.50	100.2	160.87	259.54
AA	75.83	377.0	325.13	154.1	178.76	259.92

around 50–100 °C, and at 300–350 °C (Figure 2). The thermal properties such as dehydration T_m, $\Delta_{dehydration}H$, depolymerization T_m, $\Delta_{depolymerization}H$, and glass transition temperatures $T_g(1)$ (Figures 3a and 3b) and $T_g(2)$ (Figures 4a and 4b) derived from the DSC thermograms of α-cellulose and α-cellulose-APTES are summarized in Table 4. The α-cellulose was found to have a lower value for each of the aforementioned thermal properties than α-cellulose-APTES.

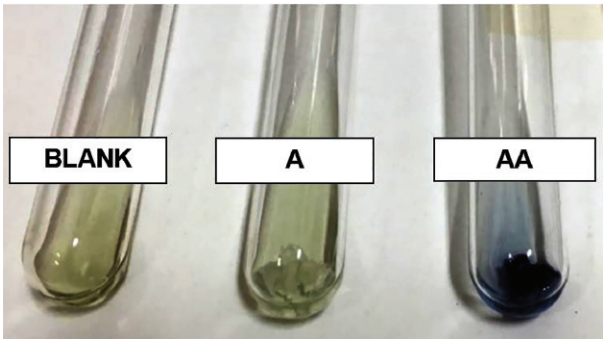

Figure 5. The reaction of α-cellulose (A) and α-cellulose-APTES (AA) with ninhydrin.

Ninhydrin Test

The reactions of α-cellulose and α-cellulose-APTES with ninhydrin were also compared. Only the α-cellulose-APTES showed a positive reaction with ninhydrin, as indicated by a purple-colored mixture (Figure 5).

DISCUSSION

Determination of the DS of α-cellulose-APTES

The DS of 0.01041 ± 0.0008 (n = 3) for α-cellulose-APTES means that there is a single substitution for every 100 β-D-glucopyranose units in cellulose. Also, the data suggest that the prepared α-cellulose-APTES may be an appropriate support for the immobilization of enzymes such as papain. It was mentioned by Agarwal (2010) that the length of a β-D-glucopyranose unit is 6.15 Å. Also, as reported by Drenth *et al.* (1962), papain has an orthorhombic crystal structure with dimensions 45.0 Å x 104.3 Å x 50.8 Å; a space group of P2,2,2; and four molecules in each unit cell. Hence, the large distance (~ 615 Å) among the APTES moieties in α-cellulose-APTES may provide ample spaces to hold papain molecules.

Optical Microscopy

The large spaces between fibers in α-cellulose-APTES (Figure 1) suggest that the hydrogen bonds among the fibers are disrupted by the incorporation of APTES to α-cellulose. Also, the swelling and ballooning of fibers (Figure 1) may be due to the use of mercerized cellulose as a starting material for the preparation of α-cellulose-APTES. Zhang *et al.* (2013) reported that the mercerization of native cellulose results in the homogeneous swelling and ballooning of fibers. Ott *et al.* (1954) observed that the radial swelling of fibers is more prominent than longitudinal swelling. They also described the ballooning of fibers, where the swelling of fibers results in the bursting of the primary layer forming a "tie" that restricts further expansion of fibers; thus, a balloon is formed.

The regeneration of α-cellulose from mercerized cellulose may have resulted in the "tying" of the disintegrated primary layers (Figure 1) due to the regeneration of hydrogen bonds. In the case of α-cellulose-APTES, the "tying" may not have occurred due to substitution with APTES in the disintegrated primary layers (Figure 1d).

ATR FTIR Spectroscopy

The similar patterns observed in the ATR FTIR transmittance spectra of α-cellulose and α-cellulose-APTES were due to the low DS of α-cellulose-APTES. The low DS agrees with the low intensity of the significant peaks which correspond to the Si-OH stretching, Si-O-Si symmetric stretching, and Si-O-C asymmetric stretching compared to the peaks from the molecular vibrations of cellulose. A similar case was observed by Loof *et al.* (2016) in silylated cellulose where the peaks for the Si-OH stretching, Si-O-Si symmetric stretching, and Si-O-C asymmetric stretching were not observed due to partial overlap with the relatively high-intensity peaks that correspond to C-H, C-O, and C-C stretches of cellulose. Loof *et al.* (2016) also reported a direct relationship between the amount of the silylating agent attached to cellulose with the intensity of the peak that corresponds to the Si-C stretching.

Ciolacu *et al.* (2011) reported that there is an agreement between the FTIR crystallinity parameters and the X-ray diffraction crystallinity indices. The LOI qualitatively describes the changes in cellulose crystallinity. The more crystalline the sample, the higher the value of LOI (Kljun *et al.* 2011). O'Connor *et al.* (1958) observed that decrystallization resulted in a decrease in the intensity of IR absorption at 1425 cm^{-1} and an increase of 898 cm^{-1}. However, the use of LOI may not be applicable to cellulose II since the partly mercerized samples did not correlate with the X-ray diffraction crystallinity measurements (Nelson and O'Connor 1964). Hence, it is also necessary to determine the TCI, the value of which is influenced by both cellulose I and cellulose II. Another parameter is the HBI, which can be associated with crystallinity based on intermolecular regularity and the presence of bound water. According to Kljun *et al.* (2011), HBI can be associated with the number of hydrogen bonds among the OH groups in cellulose. The higher HBI values may be attributed to the higher number of cellulose chains that are arranged in an organized manner, or simply the hydrogen bonds in the crystalline region (Poletto *et al.* 2014). The lower LOI and TCI of α-cellulose than that of α-cellulose-APTES suggest that α-cellulose is less crystalline than α-cellulose-APTES. The higher LOI and TCI of α-cellulose-APTES may be due to the increase in the degree of order in the amorphous region of α-cellulose upon functionalization. The introduction of new moieties in the amorphous region causes CH_2 deformation due to the increase in the frequency of interactions with the CH_2 of cellulose. In addition, the similarity between the HBI of α-cellulose and α-cellulose-APTES suggests that the functionalization of α-cellulose probably occurs in the amorphous region. The data obtained were consistent with the fact that the amorphous region in cellulose is more accessible than the crystalline region (Rowell *et al.* 2012).

Values given in Table 3 indicate that amino-functionalization has no significant effect on the O3-H --- O5' intramolecular hydrogen bonds (3342 cm^{-1}) and even on the hydrogen bonds in the phenolic groups of lignin

(3567 cm^{-1}) since there were no significant differences at 95% confidence level in the E_H and R corresponding to these hydrogen bonds in the two samples. Likewise, there was no significant difference observed in the O6-H --- O3' intermolecular hydrogen bonds (3278 cm^{-1} and 3221 cm^{-1}) between the two samples. The presence of the FTIR absorptions at 3278 cm^{-1} and 3221 cm^{-1} suggests that the samples also contain cellulose I. According to Carrillo *et al.* (2004), the presence of cellulose I can be confirmed through the IR absorptions at 1430 cm^{-1}, 1162 cm^{-1}, and 1111 cm^{-1}. The presence of these FTIR absorptions in the 2nd derivative spectra of the two samples confirms the presence of cellulose I.

According to Hebeish and Guthrie (1981), the hydroxyl group at C6 of the β-glucopyranose unit of cellulose is the most reactive among the three hydroxyl groups. The increase in E_H and decrease in R of the O2-H --- O6' intramolecular hydrogen bonds in α-cellulose-APTES may be due to the substitution of APTES in α-cellulose at C6. Dias *et al.* (2008) proved by computational and ^1H NMR experiments that hydrogen bonds between the oxygen of a silyl ether and hydrogen of alcohol [R-O-H --- O(SiR"$_3$)(R')] have higher total delocalization energies and shorter distances than hydrogen bonds between the oxygen of alcohol and hydrogen of another alcohol [R-O-H --- O(H)(R')]. They also emphasized that participation of silyl ethers in hydrogen bonds is not only due to electronic effects but also due to orbital interactions, lone pair hybridization, and lone pair energies. Based on the observations of Dias *et al.* (2008), the increase in E_H, and decrease in R of the O2-H --- O6' intramolecular hydrogen bonds in α-cellulose-APTES show that APTES was linked to the O6 of α-cellulose through silicon. Moreover, the data were consistent with the LOI and TCI values, wherein amino-functionalization results in stronger hydrogen bonds in the amorphous region.

DSC

Similar observations in the thermograms of various cellulosic samples were reported (Bertran and Dale 1986; Hirata and Nishimoto 1991; Zhang *et al.* 2013) wherein the endotherm at 50–100 °C was attributed to the dehydration or loss of water while the endotherm at 300–350 °C was due to the degradation of cellulose affording levoglucosans (Figure 2). Table 4 shows higher dehydration temperature ($T_{m\,(DH)}$) and enthalpy $\Delta_{dehydration}H$ for α-cellulose-APTES than α-cellulose. Zhang *et al.* (2013) reported that $T_{m\,(DH)}$ and $\Delta_{dehydration}H$ are inversely proportional to the tendency of the sample to dehydrate. In most cases, water is absorbed in the amorphous region. However, it is possible that the absorption of water takes place on the crystalline surfaces (Bertran and Dale 1986). Hence, the dehydration of cellulosic samples may be correlated with the crystallinity of the sample or the presence of accessible sites for water molecules. The higher value for the $T_{m\,(DH)}$ of α-cellulose-APTES may be attributed to the formation of the aminopropylsilane layer. According to Pasternack *et al.* (2008), the formation of aminopropylsilane layer may be envisioned as the formation of Si-O-Si bonds among the bound APTES molecules, and the rigid structure of the aminopropylsilane layer may cause the entrapment of some water molecules. Hence, a higher temperature is required to remove the absorbed water molecules in α-cellulose-APTES. This observation is consistent with the higher $\Delta_{dehydration}H$ of α-cellulose-APTES compared to α-cellulose, in which higher energy is required to remove water from α-cellulose-APTES.

The T_g is the temperature at half-height of the specific heat capacity change when a polymer undergoes the transition from glassy state to rubbery state (Urbaniak 2011). The reported T_g values (Figures 3 and 4) for α-cellulose and α-cellulose-APTES suggest chain lengthening due to the covalent attachment of APTES in α-cellulose-APTES. Teramoto (2015) observed the variations in the T_g of cellulose triesters of fatty acids with varying substituent chain lengths. He reported that the chain lengthening of the substituents in cellulose derivatives increases the $T_g(1)$ and decreases the $T_g(2)$.

The endotherms observed at around 300–350 °C was due to the depolymerization of the samples. According to Hirata and Nishimoto (1991), the thermal degradation of cellulose has a three-step free-radical mechanism. The three steps include the initiation or the random scission of the glycosidic linkages, grafting termination, and depropagation affording levoglucosans. The tendency of the cellulosic sample to dehydrate is inversely proportional to $T_{m\,(DP)}$ and $\Delta_{depolymerization}H$ (Zhang *et al.* 2013). Also, Sealey *et al.* (1996) reported that the increase in the side chain length of celluloses increases the $T_{m\,(DP)}$ and $\Delta_{depolymerization}H$. The higher $T_{m\,(DP)}$ of α-cellulose-APTES compared to α-cellulose is consistent with the report of Sealey *et al.* (1996).

Ninhydrin Test

The ninhydrin test involves the reaction of ninhydrin with primary amino groups to form Ruhemann's purple (Friedman 2004). Among the two samples, α-cellulose-APTES is expected to react with ninhydrin due to the presence of a primary amino group on its structure. The positive reaction of α-cellulose-APTES with ninhydrin (Figure 5) confirms the presence of a primary amino group in α-cellulose-APTES.

CONCLUSION

In this study, the amino-functionalization of α-cellulose from PCL was confirmed by optical microscopy, ATR FTIR spectroscopy, ninhydrin test, and DSC.

The prepared α-cellulose-APTES has a low DS of 0.01041 ± 0.0008 (n = 3), which suggests that it is an appropriate support for enzyme immobilization. Meanwhile, the appearance of disintegrated primary layers in α-cellulose-APTES suggests the morphological changes that occurred in α-cellulose upon treatment with APTES. The ATR FTIR data suggested that functionalization took place in the amorphous region, particularly at C6. The formation of a purple mixture upon the reaction of α-cellulose-APTES with ninhydrin suggests the presence of an amino group.

The DSC data provided additional information on the formation of Si-O-Si bonds in α-cellulose-APTES, which was indicated by higher $T_{m(DH)}$, $\Delta_{dehydration}H$, and $T_{m(DP)}$. Furthermore, the substitution of APTES in α-cellulose is indicated by the differences $T_g(1)$ and $T_g(2)$ values.

ACKNOWLEDGMENTS

The authors express their gratitude to the Department of Science and Technology – Accelerated Science and Technology Human Resource Development Program, and to the UPLB-IC FCRG.

REFERENCES

AGARWAL OP. 2010. Krishna's Organic Chemistry: Natural Products (Vol. 1), 40th ed. India: GOEL Publishing House. 82p.

ASIM M, ABDAN K, JAWAID M, NASIR M, DASHTIZADEH, Z, ISHAK MR, ENAMUL HOQUE M. 2015. A review on pineapple leaves fibre and its composites. Int J Polym Sci (Article ID 950567, 16 Pages).

BAN-KOFFI L, HAN YW. 1990. Alcohol production from pineapple waste. World J Microb Biot 6: 281–284.

BERTRAN MS, DALE BE. 1986. Determination of cellulose accessibility by differential scanning calorimetry. J Appl Polym Sci 32: 4241–4253.

BARBOSA O, ORTIZ C, BERENGUER-MURCIA A, TORRES R, RODRIGUES RC, FERNANDEZ-LAFUENTE R. 2014. Glutaraldehyde in bio-catalysts design: a useful crosslinker and a versatile tool in enzyme immobilization. RSC Adv. 4: 1583–1600.

CARRILLO F, COLOM X, SUÑOL JJ, SAURINA J. 2004. Structural FTIR analysis and thermal characterisation of lyocell and viscose-type fibres. Eur Polym J 40: 2229–2234.

CIOLACU D, CIOLACU F, POPA VI. 2011. Amorphous cellulose – structure and characterization. Cell Chem Technol 45(1–2): 13–21.

DIAS LC, FERREIRA MAB, TORMENA CF. 2008. Intra- and intermolecular hydrogen bonds in alkyl and silyl ethers: experimental and theoretical analysis. J Phys Chem A 112: 232–237.

DRENTH J, JANSONIUS JN, KOEKOEK R, MARRINK J, MUNNIK J, WOLTHERS BG. 1962. The crystal structure of papain C: I. two-dimensional Fourier synthesis. J Mol Biol 5(4): 398–407.

FRIEDMAN M. 2004. Applications of the ninhydrin reaction for analysis of amino acids, peptides, and proteins to agricultural and biomedical sciences. J Agric Food Chem 52(3): 386–406.

HEBEISH A, GUTHRIE JT. 1981. The chemistry and technology of cellulosic copolymers. New York: Springer-Verlag. 351p.

HIRATA T, NISHIMOTO T. 1991. DSC, DTA, and TG of cellulose untreated and treated with flame-retardants. Thermochim Acta 193: 99–106.

JUNG HS, MOON D, LEE J. 2012. Quantitative analysis and efficient surface modification of silica nanoparticles. J Nanomater (Article ID 593471, 8 Pages).

KLJUN A, BENIANS TAS, GOUBET F, MEULEWAETER F, KNOX P, BLACKBURN RS. 2011. Comparative analysis of crystallinity changes in cellulose I polymers using ATR-FTIR, X-ray diffraction, and carbohydrate-binding module probes. Biomacromolecules 12: 4121–4126.

KONDO T. 1997. The assignment of IR absorption bands due to free hydroxyl groups in cellulose. Cellulose 4: 281.

LIESIENE J, KAZLAUSKE J. 2013. Functionalization of cellulose: synthesis of cationic derivatives. Cellul Chem Technol 47: 515–525.

LOOF D, HILLER M, OSCHKINT H, KOSCHEK K. 2016. Quantitative and qualitative analysis of surface modified cellulose utilizing TGA-MS. Materials 9: 415.

NELSON ML, O'CONNOR RT. 1964. Relation of certain infrared bands to cellulose crystallinity and crystal lattice type. Part II. a new infrared ratio for estimation of crystallinity in celluloses I and II. J App Polym Sci 8: 1325–1341.

O'CONNOR RT, DUPRÉ EF, MITCHAM D. 1958. Applications of infrared absorption spectroscopy to investigations of cotton and modified cottons: Part I: physical and crystalline modifications and oxidation. Text Res J 28: 382–392.

OH SY, YOO II D, SHIN Y, KIM HC, KIM HY, CHUNG YS, PARK WH, YOUK JH. 2005. Crystalline structure analysis of cellulose treated with sodium hydroxide and carbon dioxide by means of X-ray diffraction and FTIR Spectroscopy. Carbohydr Res 340: 2376–2391.

OTT E, SPURLIN HM, GRAFFLIN MW. 1954. Cellulose and cellulose derivatives (Part 1). New York: Interscience Publisher. 539p.

PASTERNACK RM, AMY SR, CHABAL YJ. 2008. Attachment of 3-(aminopropyl)triethoxysilane on silicon oxide surfaces: dependence on solution temperature. Langmuir 24: 12963–12971.

POLETTO M, ORNAGHI JÚNIOR HL, ZATTERA AJ. 2014. Native cellulose: structure, characterization, and thermal properties. Materials 7(9): 6105–6119.

POPESCU C, POPESCU M, LISA G, SAKATA Y. 2011. Evaluation of morphological and chemical aspects of wood species by spectroscopy and thermal methods. J Mol Struct 988(1–3): 65–72.

PRADO KS, SPINACE MAS. 2019. Isolation and characterization of cellulose nanocrystals from pineapple crown waste and their potential uses. Int J Biol. Macromol 122: 410–416.

ROWELL RM, PETTERSEN R, HAN JS, ROWELL JS, TSHABALALA MA. 2012. Handbook of wood chemistry and wood composites, 2nd ed. USA: CRC Press. 703p.

SEALEY JE, SAMARANAYAKE G, TODO JG, GLASSER WG. 1996. Novel cellulose derivatives. IV. Preparation and thermal analysis of waxy esters of cellulose. J Polym Sci B 34: 1613–1620.

SILVA LS, FERREIRA FJL, SILVA MS, CITO AMGL, MENEGUIN AB, SABIO RM, BARUD HS, BEZERRA RDS, OSAJIMA JA, SILVA FILHO EC. 2018. Potential of amino-functionalized cellulose as an alternative adsorbent intended to remove anionic dyes from aqueous solutions. Int J Biol Macromol 116: 1282–1295.

TERAMOTO Y. 2015. Functional thermoplastic materials from derivatives of cellulose and related structural polysaccharides. Molecules 20(4): 5487–5527.

TRAN AV. 2006. Chemical analysis and pulping study of pineapple crown leaves. Ind Crop and Prod 24: 66–74.

UPADHYAY A, LAMA JP, TAWATA S. 2010. Utilization of pineapple waste: a review. J Food Sci and Technol Nepal 6: 10–18.

URBANIAK M. 2011. A relationship between the glass transition temperature and the conversion degree in the curing reaction of the EPY® epoxy system. POLIMERY 56(3): 240–243.

WU Y, JIANG Y, LI Y, WANG R. 2019. Optimum synthesis of an amino-functionalized microcrystalline cellulose from corn stalk for removal of aqueous Cu^{2+}. Cellulose 26(2): 805–821.

YU B, CHENG H, ZHUANG W, ZHU C, WU J, NIU H, LIU D, CHEN Y, YING H. 2019. Stability and repeatability improvement of horseradish peroxidase by immobilization on amino-functionalized bacterial cellulose. Process Biochem 79: 40–48.

ZHANG S, WANG W, LI F, YU J. 2013. Swelling and dissolution of cellulose in NaOH aqueous solvent systems. Cell Chem Technol 47(9–10): 671–679.